International Journal of Pharmaceutics 436 (2012) 248–257

Contents lists available at SciVerse ScienceDirect

International Journal of Pharmaceutics

journal homepage: www.elsevier.com/locate/ijpharm

Pharmaceutical Nanotechnology

An arginine derivative contained nanostructure lipid carriers with pH-sensitive membranolytic capability for lysosomolytic anti-cancer drug delivery

Sai Li[a], Zhigui Su[a], Minjie Sun[a], Yanyu Xiao[a], Feng Cao[a], Aiwen Huang[a,b], Hongying Li[a,c], Qineng Ping[a,*], Can Zhang[a,**]

[a] Department of Pharmaceutics, Key Lab of State Natural Medicine, China Pharmaceutical University, Nanjing 210009, PR China
[b] Department of Pharmacy, Fuzhou Jeneral Hospital of Nanjing Military District, Fuzhou 350025, PR China
[c] Department of Pharmacy, Disha Pharmaceutical Group, Weihai 264205, PR China

ARTICLE INFO

Article history:
Received 11 April 2012
Received in revised form 1 June 2012
Accepted 15 June 2012
Available online 23 June 2012

Keywords:
L-Arginine lauril ester
pH-sensitive
Lysosomolytic
Nanostructure lipid carriers
Bovine serum albumin
Paclitaxel

ABSTRACT

By inserting L-arginine lauril ester (AL) into nanostructure lipid carriers (NLCs) and then coating with bovine serum albumin (BSA), pH-sensitive membranolytic and lysosomolytic nanocarriers (BSA-AL-NLCs) were developed. Hemolysis assay demonstrated the pH-sensitive biomembrane disruptional capability of AL and BSA-AL-NLCs. BSA-AL-NLCs did not disrupt biomembrane at pH 7.4 even at high concentration, exhibited ideal feasibility as lysosomolytic drug delivery nanoparticles without cytotoxicity. Confocal Laser Scanning Microscope (CLSM) images confirmed the lysosomolytic capability of BSA-AL-NLCs after internalized into MCF-7 (human breast cancer cell) via endosome–lysosome path in vitro. Paclitaxel (PTX) loaded BSA-AL-NLCs displayed pH-dependent release in vitro. In MCF-7 viability test with MTT assays, both the blank NLCs did not exhibit cellular toxicity. Of particular interest, the in vitro cell experiments demonstrated that the anti-tumor effect of PTX-loaded BSA-AL-NLCs was preferable to BSA-NLCs, even comparable with PTX solution, which indicated that AL served to facilitate lysosomal escape of BSA-AL-NLCs so as to improve the anti-cancer effect. Biodistribution and anti-cancer activity in vivo confirmed the improved tumor targeting and anti-cancer efficacy of BSA-AL-NLCs. The study suggested that the simple and small molecule of AL may render more nanocarriers lysosomolytic capability with lower cytotoxicity, as well as improved therapeutic index of loaded active agents.

1. Introduction

As nano-drug delivery systems (NDDSs) have been widely researched, more and more attentions were paid to their intracellular fate. Amounts of NDDSs internalize cells via endosome–lysosome path (Sahay et al., 2010), while lysosome, an organelle encapsulates acidic cytoplasm containing many types of enzymes, may induce degradation of NDDSs and its loaded active drugs. Unfortunately nanocarriers without special function lack the ability to escape from endosome–lysosome timely, resulting in poor therapeutic index of the loaded active agents (Singh et al., 2008; Van den Bossche et al., 2011). Therefore, endo/lysosomal escape is fundamental for drugs sensitive to lysosomal degradation or that needs to reach extra endo/lysosomal targets (Paillard et al., 2010).

Many endo/lysosomal escape approaches depending on the weak acidic environment have been reported, which could be summarized in three aspects. The first strategy was using cationic polymers with the characterization named "Proton Sponge Effect". When nanocarriers composed of these cationic polymers entered lysosome, amounts of proton were adsorbed and induced Cl^- influxing and accumulation, resulting osmotic swelling and final lysosome leak/lysis (Kichler et al., 2001). Among these cationic polymers, such as polyethylenimine (PEI) (Boussif et al., 1995), polylysine (Meyer et al., 2007), poly(β-amino esters) (Tzeng et al., 2011), PEI was the most efficient agent for lysosomal escaping. However, these cationic polymers caused high cytotoxicity to cells for strong positive charge and nondegradable in vivo (Fischer et al., 1999). Some modification, such as conjugating branches to these polymers, could reduce the cytotoxicity, while the lysosomolytic capability was decreased (Kim et al., 2004; Masotti et al., 2007).

The second strategy was adding fusogenic lipid or fusogenic peptide, called "helper lipid", in liposomes formulation to facilitate their endo/lysosomal escape (Wang et al., 2010). Fusogenic lipid or fusogenic peptide mimicked the fusion of viral envelopes with host cell endosome membranes during viral infections (Martin and Rice, 2007). Dioleoyl-phosphatidylethanolamine (DOPE) was the

* Corresponding author. Tel.: +86 25 83271092; fax: +86 25 83271092.
** Co-corresponding author. Tel.: +86 25 83271171; fax: +86 25 83271171.
E-mail addresses: pingqn2004@yahoo.com.cn, Pingqn2008@yahoo.com.cn (Q. Ping), canzhang65@yahoo.com.cn (C. Zhang).

0378-5173/$ – see front matter © 2012 Elsevier B.V. All rights reserved.
http://dx.doi.org/10.1016/j.ijpharm.2012.06.040

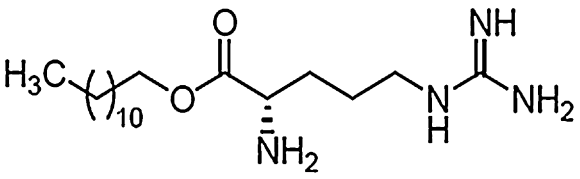

Fig. 1. Chemical structure of AL.

representative "helper lipid". It has been suggested that under mild acidic environment of endosome–lysosome, DOPE might induce fusion between DOPE composed liposome and endosome–lysosome membrane, resulting the leakage of entrapped agents to cytoplasm (Mui et al., 2000; Vanić et al., 2011). However, the high cost or complex synthesis procedure limited the application of fusogenic lipid or fusogenic peptide.

The third strategy was to prepare nanoparticles using pH-sensitive membranolytic materials to acquire endo/lysosomolytic capability (Yessine and Leroux, 2004). Following cell uptake and trafficking to endo/lysosome, these materials could be triggered by endo/lysosomal pH and undergo a change from hydrophilic to hydrophobic form, which was membrane-disruptive. This form induced endo/lysosome membrane disruption and promoted endo/lysosomal escape of these nanocarriers (Yessine and Leroux, 2004). pH-responsive membranolytic polyanions, including polymalic acid (Ding et al., 2011), Poly(alkylacrylic acid) (Jones et al., 2003), poly(L-lysine iso-phthalamide) (Chen et al., 2008; Eccleston et al., 2000; Khormaee et al., 2010), were widely used to prepare endo/lysosomolytic nanocarriers. Structural optimization of these polyanions improved their pH-sensitive membranolytic activity and drug loading capability. For example, grafting hydrophobic amino acid chain to poly(L-lysine iso-phthalamide) enhanced its membrane disruption activity (Chen et al., 2009a,b; Ho et al., 2011). Charge neutralization of polymalic acid by substituting pendent carboxylates with hydrophobic amino acid derivatives, improved its affinity with membranes and acquired membranolytic activity of hydrophobic residues (Ding et al., 2011). Recently, some pH-sensitive membranolytic surfactants were used to form self-assembled lysosomolytic micelles. N-(1-aminoethyl)iminobis [N-(oleicyl-cysteinyl-histinyl-1-amino-ethyl)propionamide] (EHCO) and its optimized derivatives, amphiphilic surfactants with pH-sensitive hemolytic ability, were synthesized and used to prepare micelles which could disrupt lysosome and diffuse to cytoplasm rapidly (Wang et al., 2007, 2009; Xu et al., 2010a). Hemolytic assay demonstrated its high hemolytic activity at endo/lysosomal pH, which caused endo/lysosomolysis. These endo/lysosomolytic materials were able to facilitate the transportation from endo/lysosome to cytoplasm, but are still suffered from some disadvantages. Net negative charged polyanions showed decreased cellular binding due to the electrostatic repulsion with anionic cell membrane (Ding et al., 2011). EHCO and its derivatives were difficult to gain for complex synthesis procedures were required (Wang et al., 2007).

Except the disadvantages mentioned above, these materials were only used to form self-assembling nanocarriers or prepare liposomes, which meant their applicability in lysosomolytic research was very limited. While endo/lysosomes induce damage to all nanocarriers that entry cells through endosome–lysosome path (Yessine and Leroux, 2004), endo/lysosomal escape is necessary for these nanocarriers to protect nanocarriers and loaded cargos. To address those concerns, we planned to find a pH-sensitive membranolytic substance which could be readily incorporate into various nanocarriers and render them lysosomolytic capability.

L-Arginine lauril ester (AL, Fig. 1), an arginine derivant, was first synthesized as a relaxant inhibitor (Wang et al., 2004). It contains a hydrophobic chain and a hydrophilic head group with protonatable amino groups, including the primary and secondary amines which would be protonated at acidic and neutral pH, respectively. This special structure attracted us to confirm whether it was pH-sensitive biomembranolytive. Herein we report the pH-sensitive membrane disruptional capability of AL and its composed nanocarriers that can be used for lysosomolytic drug delivery. Bovine serum albumin (BSA) coated nano-structure lipid carriers containing AL, BSA-AL-NLCs, were prepared according to our early research (Xu et al., 2010b), where BSA was used as the model protein to mimic the shell of lipoproteins and can be modified with ligand group to target cancer cells. Here, BSA was coated on the nanocarriers to shield the strong positive charge and reduce the potential cytotoxicity and prolong resistance time in blood. Hemolysis assay was taken to certify pH-sensitive membranolytic capability both of AL and BSA-AL-NLCs. We have characterized these NLCs by dynamic light scattering (DLS), atomic force microscopy (AFM), transmission electron microscopy (TEM), and surface charge (zeta potential) measurements. Lysosomolytic activity of BSA-AL-NLCs in MCF-7 cells was confirmed by Confocal Laser Scanning Microscope (CLSM), and the in vitro anti-tumor effects of paclitaxel-loaded nanocarriers were studied using MTT assay. Biodistribution and in vivo anti-tumor research were employed to confirm the tumor targeting and cancer inhibition efficacy of BSA-AL-NLCs.

2. Materials and methods

2.1. Materials

L-Arginine was a kind donation from Ajinomoto Amino Acid Co. Ltd. (Shanghai, China). Laurinol was supplied by Yonghua Co. (Jiangsu, China). Medium chain triglycerides (LIPOID MCT) were purchased from Lipoid GMBH. Phosphatidylcholine (LIPOID S100) was obtained from Toshisun Co. BSA was purchased from Sunshine Biotech Co. Ltd. (Shanghai, China). Dulbecco's modified Eagle's medium (high glucose) cell culture medium (DMEM-HG) was obtained from Gibco (Life Technologies, Switzerland). All other chemicals, reagents, and solvents were analytical grade otherwise stated.

2.2. Synthesis of AL

AL was synthesized through a simple one-step chemical reaction according to procedures previously reported with some adjustment (Wang et al., 2004). Briefly, L-arginine (1.0 g) was suspended in laurinol (hydrogen chloride saturated, 15 mL). The mixture was heated up to 100–110 °C (oil bath) for 15 min and filtrated to remove the unreacted Arginine. Unreacted laurinol was washed away using dichloromethane as eluant on SiO_2 column chromatography, then washed AL down using methanol as eluant and collected. Methanol was removed by vacuuming and AL was finally obtained.

2.3. Preparation of blank or calcein/PTX-loaded BSA-NLCs and BSA-AL-NLCs

BSA-NLCs and BSA-AL-NLCs were prepared as previously described by our group with some adjustment (Xu et al., 2010b). PC, MCT with or without AL were dissolved in methanol and dried under reduced pressure at 30 °C to remove the solvent. The dried film was redispersed in BSA solution. The suspension was sonicated under 200 W at 4 °C for 5 min, followed by extruding through 0.22 μm filters multiple times to obtain the final BSA-NLCs or BSA-AL-NLCs. Calcein/PTX-loaded NLCs were prepared using the same method by adding calcein/PTX to the lipid mixture solution. The loading efficiencies of PTX or calcein in both NLCs were similar, about 4% and 0.1%, respectively.

Although BSA did not adsorb to NLCs without AL, BSA was added in the hydrate solution to certify hemolysis and lysosomolytic ability of BSA-AL-NLCs was offered by AL but not BSA. The obtained NLCs were named BSA-NLCs even without BSA layer on the surface.

2.4. Hemolysis assay of AL and NLCs

Blood from rat was centrifuged at 1000 × *g* for 5 min to isolate Erythrocytes (RBC). The cell pellets were resuspended into a 2% (w/v) RBC solution with isotonic phosphate buffered saline (PBS) at appropriate pH (pH 5.4, 6.5 or 7.4) and then seeded (100 μL) into a 96-well plate. 100 μL of AL solution (different pH PBS was used as solvents) was added to RBC solutions in triplicates and the plate was incubated for 1 h at 37 °C. Triton X-100 (2%, w/v) and isotonic PBS of different pH were used as positive and negative control, respectively. The absorbance of the supernatant from each sample was measured at 570 nm using a micro-plate reader. The relative hemolytic activity of AL was calculated by

$$\frac{\mathrm{Abs_{sample}} - \mathrm{Abs_{buffer}}}{\mathrm{Abs_{Triton}} - \mathrm{Abs_{buffer}}} \times 100\% \quad (1)$$

where $\mathrm{Abs_{sample}}$, $\mathrm{Abs_{buffer}}$ and $\mathrm{Abs_{Triton}}$ stand for the absorbance intensity of RBC treated with NLCs, PBS and Triton X-100, respectively.

The hemolysis assay of NLCs was similar to AL with some additional operation: the supernatant from each sample after incubation should be treated with 100 μL 2% Triton X-100 and centrifuged again to avoid absorption of nanoparticles in the supernatant at determine wavelength.

2.5. Size and zeta potential measurement of NLCs

100 μL of NLCs was diluted to 4 mL using deionized water, and then particle size and zeta potential were measured by using Zetaplus (Brookhaven Instruments, UK) at 25 °C.

2.6. TEM and AFM imaging

Morphological examination of PTX-loaded NLCs was performed under transmission electron microscopy (TEM, H-7650, Hitachi High-Technologies Corporation) and Atomic Force Microscopy with tapping model (AFM, Nanoscope V Bioscope™, Veeco Instruments).

2.7. In vitro release of PTX from NLCs

Release experiments of PTX from the nanoparticles in vitro were performed by dialysis of the PTX-loaded NLCs in PBS of different pH containing 0.1% Tween 80. PTX-loaded NLCs suspension was diluted 10 times by adding 4.5 mL PBS at appropriate pH to 0.5 mL NLCs. Then, 0.5 mL diluted NLCs were placed in dialysis bags (10,000 Da molecular weight cut-off). Next, dialysis bags were incubated in 100 mL of PBS at 37 °C and shaken at 100 rpm. Samples (1.0 mL) were withdrawn at fixed time and fresh buffer was added. Samples were centrifuged at 12,000 rpm for 5 min and the supernatant was determined by HPLC method.

Release experiments of PTX in dialysis medium with changed pH were carried out to evaluate the release of PTX under Intracellular environments. The operation was similar with the method above except replace PBS of pH 5.4 with PBS of pH 7.4 at 1 h.

2.8. Ablation of BSA from BSA-AL-NLCs at different pH

1 mL BSA-AL-NLCs was added to 4 mL PBS of pH 5.4, pH 6.5 and pH 7.4 and incubated for 30 min under slight stirring at room temperature. Then, 1 mL sample was taken out to separate free BSA from NLCs and the concentration of free BSA was detected by BCA method (Smith et al., 1985). The ablate ration (AR) of BSA from BSA-AL-NLCs was calculated by

$$\mathrm{AR} = \frac{\mathrm{BSA_{free}}}{\mathrm{BSA_{tot}}} \times 100\% \quad (2)$$

where $\mathrm{BSA_{free}}$ and $\mathrm{BSA_{tot}}$ stand for the amount of free and total BSA in the NLCs suspension, respectively.

2.9. Cell culture

MCF-7 (human breast cancer) cell was cultured in DMEM-HG supplemented with 10% inactivated fetal bovine serum (FBS), penicillin (100 U/mL) and streptomycin (100 μg/mL) at 37 °C in an incubator (Thermo Electron Corporation) with 5% CO_2. The cells were harvested with 0.025% trypsin and rinsed. The resulted cell suspension was used in the following experiments.

2.10. CLSM imaging

Calcein-loaded AL-NLCs was prepared according to Section 2.3 using distilled water instead of BSA solution to hydrate the AL-contained lipid film. Its particle size, zeta potential and calcein loading efficiency were 69.9 nm, +12.5 mV and about 0.1%, similar to that of BSA-NLCs and BSA-AL-NLCs.

MCF-7 cells were seeded in cell culture dish (Costar, USA) at a density of 10,000 cells/dish and incubated in 1 mL complete medium for 24 h. After incubated with DMEM-HG (without FBS, pH 7.4) for 20 min, 500 μL BSA-NLCs, BSA-AL-NLCs or AL-NLCs were added to replace DMEM-HG and incubated for another 1 h. The sample was replaced with 500 μL DMEM-HG and incubated for another 0 h, 1 h and 3 h respectively. After the culture medium was removed and the dishes were rinsed with PBS (pH = 7.4), Lyso-tracker red was added to stain the lysosomes and culture media were replaced with PBS. A confocal laser scanning microscope (CLSM, Olympus FV300-BXCarl Zeiss LSM-410, Tokyo, Japan) was used to exam the cells after incubation.

2.11. Cytotoxicity

The cytotoxicity of prepared NLCs was evaluated by determining the cell viability using MTT assays. The cells (MCF-7 cells) were seeded in 96-well plates at a density of 5×10^3 cells/well and incubated in 200 μL complete medium for 24 h. Then, the medium was replaced by BSA-NLCs or BSA-AL-NLCs samples diluted in DMEM-HG (without FBS, pH 7.4) and incubated for another 24 h. At given time intervals, 10 μL of MTT (5 mg/mL in pH 7.4 PBS) was added and incubated for 4 h in incubator. 150 μL DMSO was added to replace the medium in order to solubilize the formazan crystals. The UV absorbance intensity was measured by Microplate Reader (Thermo Electron Corporation) at λ = 570 nm. Each point was performed in triplicates. Cell viability was calculated by the following equation

$$\text{Cell viability} = \frac{\mathrm{OD_s}}{\mathrm{OD_{control}}} \times 100\% \quad (3)$$

where $\mathrm{OD_s}$ stands for the absorbance intensity of the cells treated with NLCs, while $\mathrm{OD_{control}}$ stands for the absorbance intensity of the cells incubated with culture medium.

2.12. In vitro anti-tumor assay

MCF-7 cells (5×10^3 cells/mL) were harvested and seeded in 96-well plates with 200 μL of DMEM-HG medium for 24 h. PTX solution and PTX-loaded NLCs in DMEM-HG were added to the

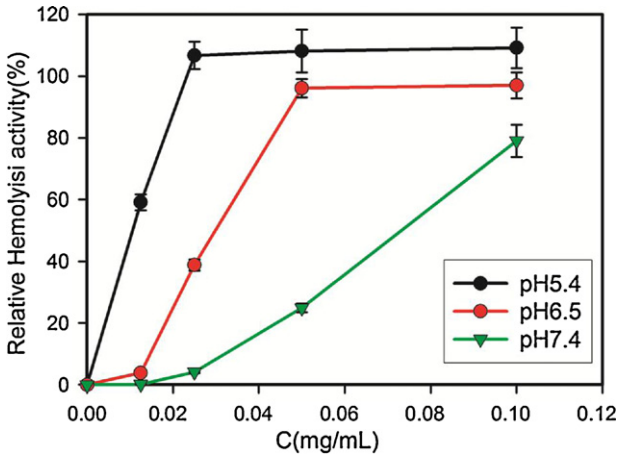

Fig. 2. Hemolytic activity of AL in the PBS media of pH 5.4, pH 6.5 and pH 7.4. Triton X-100 and PBS of different pH were used as positive and negative control, respectively. Mean and S.D. are shown ($n = 3$).

medium-removed 96-well plates with different PTX concentrations and incubated for 48 h. 10 μL of MTT (5 mg/mL in pH 7.4 PBS) was added after the wells were rinsed with PBS (pH7.4). After incubated for additional 4 h, 150 μL DMSO was added to replace the medium in order to solubilize the formazan crystals. The absorbance was measured by Microplate Reader at $\lambda = 570$ nm. Cell viability was calculated according to Eq. (3).

2.13. Biodistribution

All experiments involving animals were approved by the University Ethics Committee for the use of experimental animals and carried out according to the National Institute of Health Guide for the Care and Use of Laboratory.

Male Kunming mice were inoculated subcutaneously in the right armpits with 0.1 mL S-180 cell suspension (4×10^6) to establish tumor-bearing mice. Once the tumor volume reached about 200 mm^3, the mice received intravenous injection, via the tail vein, of BSA-AL-NLCs, BSA-NLCs or Taxol at a PTX dose of 15 mg/kg. Mice were exsanguinated through femoral artery at 10 min, 30 min, 1 h, 2 h, 6 h and 12 h post-injection (3 mice for each time point). The heart, liver, spleen, lung, kidney and tumor were collected and weighted. Blood and tissue samples were placed separately in vials and stored at −20 °C.

0.1 mL blood samples or and 0.8 mL tissue homogenate was mixed with 10 μL of internal standard (Diazepam, 27 μg/mL) and extracted with 4 mL of tetra-butyl methyl ether. The clear supernatant was removed after centrifugation at 4000 rpm for 10 min and evaporated under reduced pressure. The residue was then dissolved by 200 μL of mobile phase and centrifuged at 12,000 rpm for 5 min before HPLC analysis.

2.14. In vivo anti-tumor activity

Male Kunming mice were inoculated subcutaneously in the right armpits with 0.1 mL S-180 cell suspension (4×10^6) to establish tumor-bearing mice. On day 2 (the day of tumor inoculated was assigned as day 0), the mice were weighed and randomly divided into four groups ($n = 5$). The control saline or preparations (Taxol, BSA-AL-NLCs, BSA-NLCs) were intravenously administered via the tail vein at a dose of 15 mg/kg every 2 days for 5 times. The body weight of mice was weighed everyday. At day 11, all mice were sacrificed and the tumor mass was removed, photographed and weighted. Change ratio of body weight was calculated by dividing by the weight at day 1. Anti-tumor efficacy was evaluated by tumor inhibition rate (TIR), which was calculated according to the

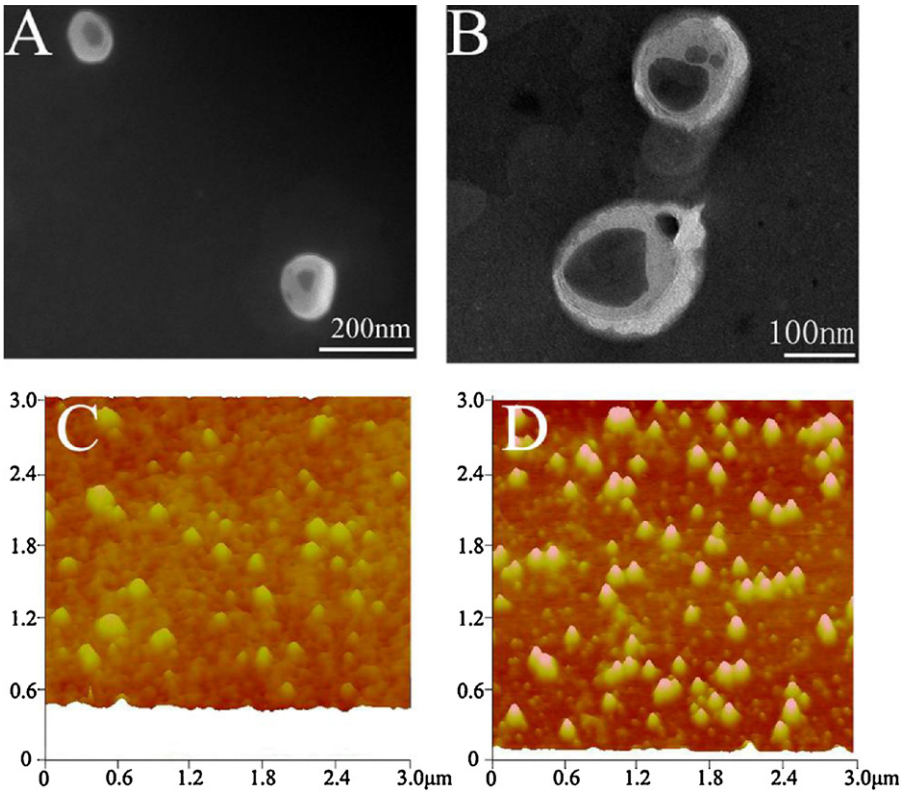

Fig. 3. (A) TEM and (C) AFM images of BSA-NLCs; (B) TEM and (D) AFM images of BSA-AL-NLCs. Both of the particles were prepared with similar loading efficiencies of PTX.

following equation.

$$\text{TIR} = \frac{\text{tumor weight of saline group} - \text{tumor weight of treated group}}{\text{tumor weight of saline group}} \times 100\% \quad (4)$$

2.15. Statistical analysis

Both ANOVA and Student's two-sample *t*-test were utilized for statistical evaluation. $P < 0.05$ was considered significant.

3. Results

3.1. Hemolysis assay of AL

Hemolysis assay was employed to evaluate the pH-sensitive membranolytic capability of AL. Fig. 2 showed the hemolysis activity of AL in PBS of different pH. AL exhibited both concentration-dependant and pH-dependant hemolysis activity. At the concentration around 0.025 mg/mL, AL showed negligible hemolysis at pH 7.4 (physiological pH), about 40% hemolysis ability at pH 6.5 (endosomal pH), and almost complete hemolysis ability at pH 5.4 (lysosomal pH). It could be drawn from the results that around this concentration, AL was membranolytic only at lysosomal pH.

3.2. Size and zeta potential of BSA-NLCs and BSA-AL-NLCs

It should be declared that 2.5 mg/mL BSA solution was used to hydrate the lipid film based on our previous study.

The size of BSA-NLCs prepared without AL was 72.2 nm. Compared with BSA-NLCs, BSA-AL-NLCs showed increased mean diameter, about 80 nm, due to BSA coated efficiently on the surface of AL-NLCs. Both the NLCs with or without BSA coating layer were smaller than 100 nm that difference of size would not affect their internalization and fate in cell.

BSA-NLCs exhibited a weak negative zeta potential around −2 mV, while BSA-AL-NLCs was positive charged, judging from its zeta potential of +5.02 mV. Without BSA coating layer, the zeta potential of AL-NLCs was stronger (about +12.5 mV). In this study, BSA was added to shield the strong positive potential partly to increase the stability and prolong the resistance time in blood.

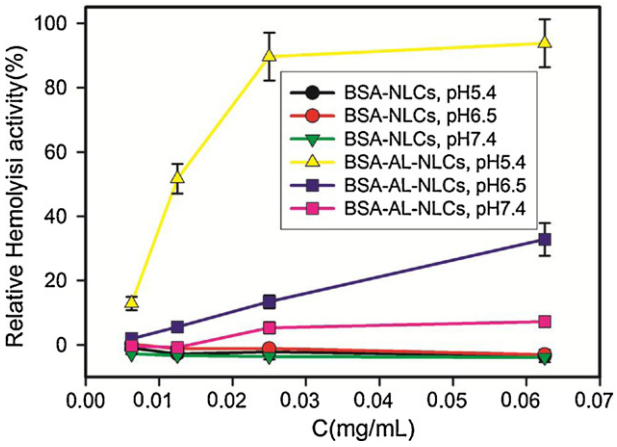

Fig. 4. Hemolytic activity of BSA-NLCs and BSA-AL-NLCs in PBS of pH 5.4, pH 6.5 and pH 7.4. The concentration of NLCs was shown as the concentration AL. Triton X-100 and PBS of different pH were used as positive and negative control, respectively. Mean and S.D. are shown ($n = 3$).

3.3. TEM and AFM imaging

TEM of BSA-NLCs and BSA-AL-NLCs were shown in Fig. 3 and most of them showed regular, spherical morphous shape. Fig. 3A showed smooth appearance of NLCs, while Fig. 3B clearly displayed the BSA layer on BSA-AL-NLCs. In AFM images Fig. 3C and D, BSA-AL-NLCs looked brighter at the central of particles than BSA-NLCs, standing for higher height of BSA-AL-NLCs in comparison with BSA-NLCs. The apparent size of TEM and AFM images were slightly larger than measured size using DLS analyzer.

3.4. Hemolysis assay of NLCs

Hemolysis assay was also done to evaluate the pH-sensitive membranolytic activity and predict the lysosomolytic capability of BSA-AL-NLCs. As Fig. 4 showed, BSA-NLCs exhibited negligible hemolytic capability at the whole concentration and pH range. BSA-AL-NLCs displayed negligible hemolytic activity at pH 7.4 even at the highest concentration. When pH decreased to 6.5, hemolytic capability of BSA-AL-NLCs increased along with the raise of AL concentration. At pH 5.4, BSA-AL-NLCs showed stronger hemolytic capability than pH 7.4 and 6.5 ($P < 0.05$), while complete hemolysis was achieved when the AL concentration was above 0.025 mg/mL. This result indicated BSA-AL-NLCs were membranolytic only at acidic pH even at high concentration.

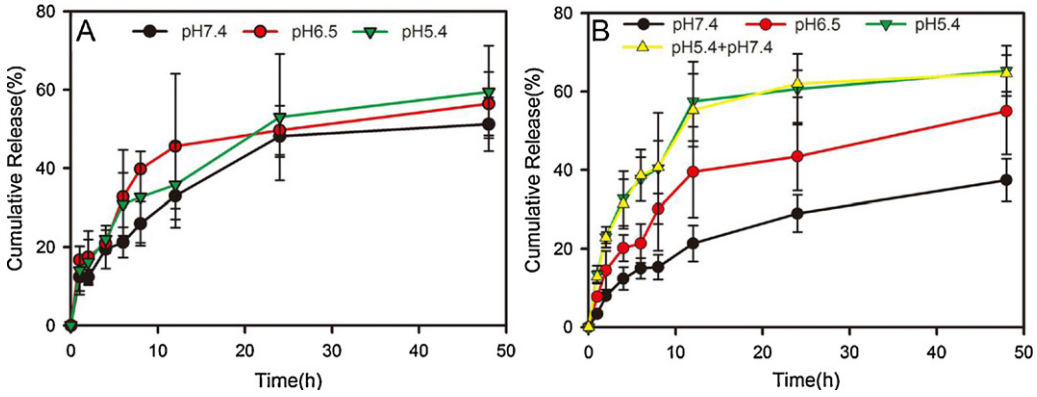

Fig. 5. Release profiles of PTX from BSA-NLCs (A) and BSA-AL-NLCs (B) at 37 °C in PBS with different pH. The yellow curve displayed the release profile of PTX from BSA-AL-NLCs at pH 7.4 after dialyzed in PBS of pH 5.4 for the first 1 h. Mean and S.D. are shown ($n = 3$). (For interpretation of the references to color in this figure legend, the reader is referred to the web version of the article.)

3.5. In vitro release of PTX from NLCs

The entrapment efficiency of PTX in BSA-NLCs and BSA-AL-NLCs were 97.2 ± 2.3% and 97.6 ± 1.5%, respectively. Fig. 5 displayed the release profiles of PTX from BSA-NLCs and BSA-AL-NLCs in PBS of different pH. There was no significant difference between the release of PTX from BSA-NLCs at different pH ($P > 0.05$), Fig. 5A. In contrast, the release from BSA-AL-NLCs increased when pH decreased from 7.4 to 5.4, as shown in Fig. 5B. The release of PTX from BSA-AL-NLCs was rather slow at pH 7.4, reached a cumulative release of 28.9% for 1 day and 37.4% for 2 days. However, at pH 5.4, a noticeably increased release of PTX was observed with about 40% within 8 h and 65.3% after 2 days.

Further study of the release properties under changed pH was carried out to simulate intracellular process after endocytosis. As Fig. 5B (yellow curve) showed, BSA-AL-NLCs displayed greatly increased release at pH 7.4 after dialyzed at pH 5.4 for the first 1 h. The total cumulative release achieved 59.3%, close to the total cumulative release at pH 5.4 (65.3%). The temporary retention at pH 5.4 raised the release of PTX from BSA-AL-NLCs at pH 7.4 significantly.

3.6. Ablation of BSA from BSA-AL-NLCs at different pH

The ablate ratio of BSA from BSA-AL-NLCs at pH 7.4, pH 6.5 and pH 5.4 was 6.75 ± 3.17%, 14.60 ± 5.74% and 86.62 ± 14.35%, respectively. This result indicated that more BSA ablated from BSA-AL-NLCs with the decrease of pH. Amounts of BSA ablated at pH 5.4 even after only 30 min incubation.

3.7. CLSM imaging

Calcein, a pH-responsive fluorescent probe emerges green fluorescence at natural pH and undergo self-quenching in acid environment (Ho et al., 2011; Jones et al., 2003), was chosen to trace the locus of NLCs in cells. Lysosomolytic ability of AL-NLCs was also studied to verify BSA layer on BSA-AL-NLCs did not contribute to lysosome escape, as well as did not reduce lysosomal disrupt activity. Fig. 6 clearly displayed the cytoplasmic locus of calcein labeled NLCs (green) in MCF-7. Amounts of lysosomes appeared in cells after incubate with NLCs for 1 h due to the internalization of BSA-NLCs, BSA-AL-NLCs or AL-NLCs via endosome–lysosome path.

In cells administrated with BSA-NLCs, lysosomes did not decrease as time proceeded, meanwhile, green fluorescence of calcein did not increase. These indicated that lysosomes were unbroken and calcein-loaded BSA-NLCs were still entrapped in lysosomes. When incubated with BSA-AL-NLCs or AL-NLCs, red fluorescence of lysosomes decreased continually and green fluorescence of calcein in cytoplasm increased expressly, indicating the unassailable lysosomolytic activity induced by BSA-AL-NLCs/AL-NLCs and the diffusion of BSA-AL-NLCs/AL-NLCs into cytoplasm.

3.8. Cytotoxicity and in vitro anti-tumor assay

As shown in Fig. 7A, blank NLCs either with or without AL, did not exhibit cellular toxicity as determined by MTT assay. This is especially beneficial for the NLCs to be used as Intracellular drug delivery nanoparticles without nonspecific cytotoxicity.

As shown in Fig. 7B, PTX-loaded BSA-AL-NLCs exerted higher cytotoxicity compared with BSA-NLCs. For example, at the concentration of 5 μg/mL, PTX-loaded BSA-NLCs and BSA-AL-NLCs reduced the cell viability with very significant difference ($P < 0.001$), by 47.7% and 81.4%, respectively. However, both NLCs showed lower cytotoxicity than PTX solution, which enabled 94.6% reduction in cell viability at this concentration. Conclusion could be made

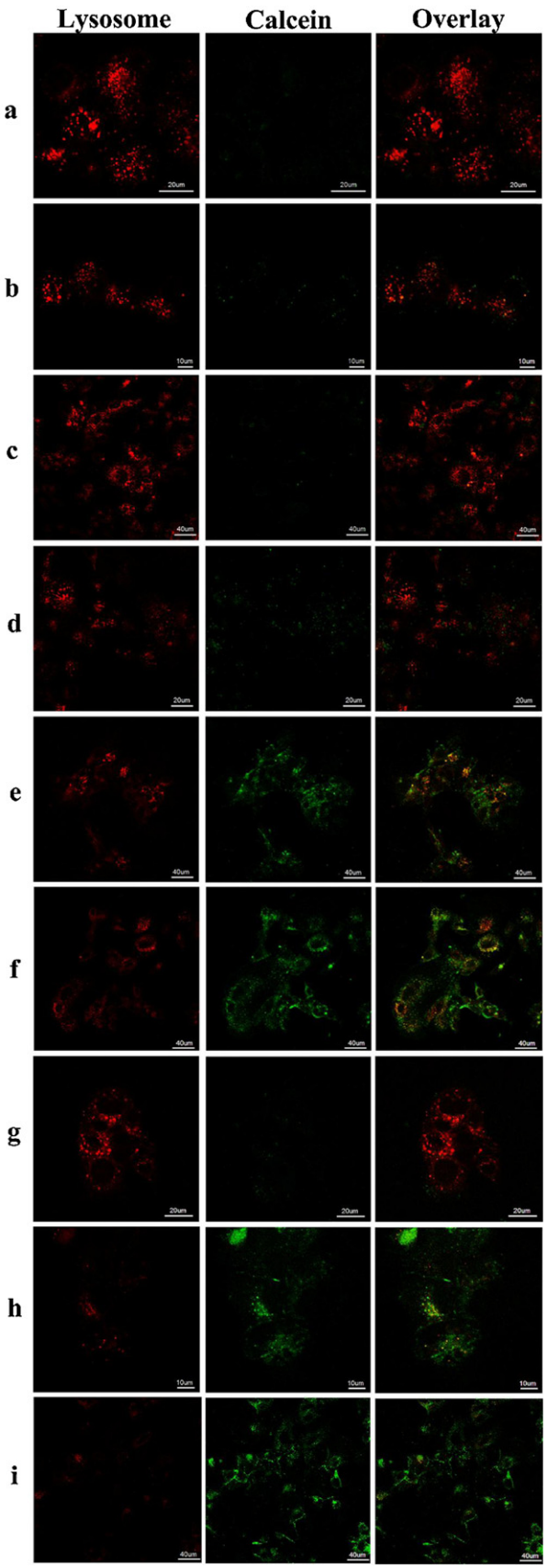

Fig. 6. Confocal images of MCF-7 at 0 h, 1 h, 3 h after incubated with calcein loaded BSA-NLCs (a–c), BSA-AL-NLCs (d–f) and AL-NLCs (g–i) for 1 h at first. Lysosomes (red) was stained with lyso-tracker red, green fluorescence stood for calcein loaded NLCs. (For interpretation of the references to color in this figure legend, the reader is referred to the web version of the article.)

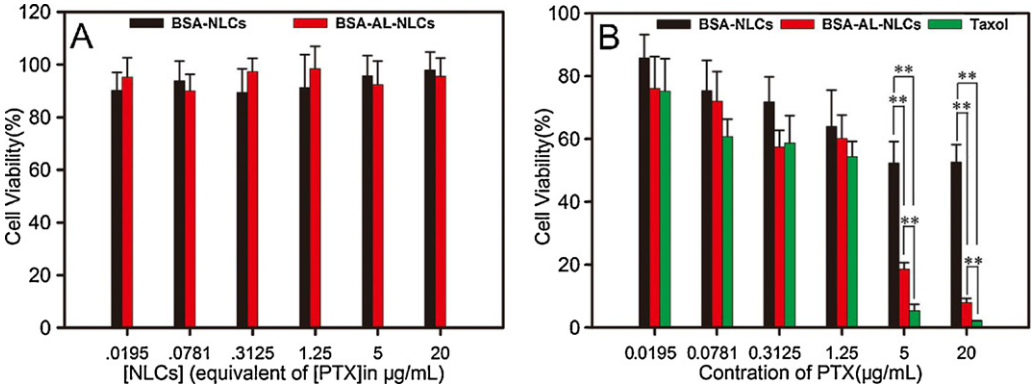

Fig. 7. The cell cytotoxicity (MCF-7) of blank NLCs (24 h, A) and in vitro anti-tumor effect of PTX loaded NLCs with different concentrations (B, 48 h). Mean and S.D. are shown ($n = 3$).

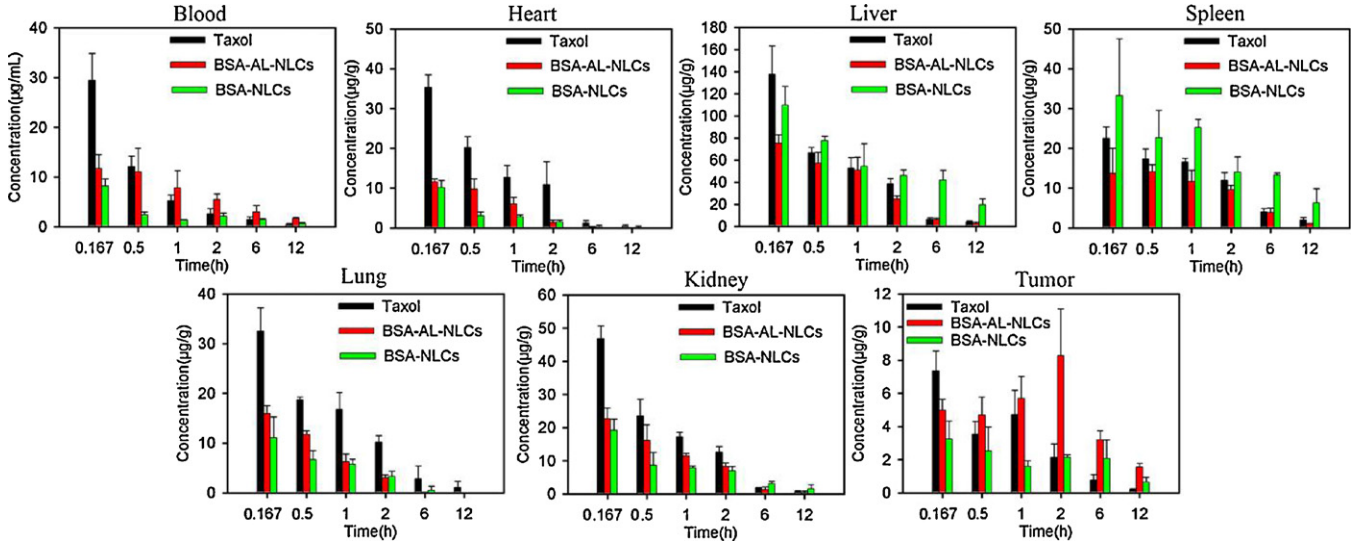

Fig. 8. Biodistribution profile of Taxol and PTX-loaded NLCs after intravenous injection at the dose of 15 mg/kg.

that BSA-AL-NLCs was more effective to inhibit the proliferation of tumor cells than BSA-NLCs.

3.9. Biodistribution

Fig. 8 presented the mean concentrations of PTX in tissues of tumor-bearing mice after intravenous injection. From this data, it appeared that Taxol was cleared rapidly in plasma and tissues, while PTX-loaded NLCs showed prolonged residence time in blood and tissues. It was obviously that most of Taxol and PTX-loaded NLCs accumulated at liver. BSA-NLCs showed better targeting ability to liver and spleen compared with BSA-AL-NLCs. After injection of Taxol and BSA-NLCs, the highest concentration of PTX in tumor tissue appeared at 10 min and decreased to 0.19 μg/g and 0.65 μg/g at 12 h, respectively. In comparison, PTX achieved the highest concentration at 2 h post-injection of BSA-AL-NLCs due to the accumulation of NLCs caused by EPR effect. PTX concentration was about 1.56 μg/g even 12 h after injection, much higher than that of Taxol and BSA-NLCs. This indicated the accumulation and prolonged residence of PTX-loaded BSA-AL-NLCs in tumor in comparison with Taxol and BSA-NLCs. Table 1 displayed the AUC_{0-t} of PTX in blood and other tissues after intravenous injection. It was obviously that the AUC_{0-t} of BSA-AL-NLCs in blood was 1.39-fold and 2.50-fold higher than that of Taxol and BSA-NLCs, while in tumor was 2.95-fold and 2.33-fold higher, respectively. However, BSA-NLCs exhibited the best targeting ability in liver and spleen, judging from the 2.11-fold and 2.79-fold higher AUC_{0-t} in liver and 1.97-fold and 2.52-fold higherAUC_{0-t} in spleen than that of Taxol and BSA-AL-NLCs, respectively. BSA-AL-NLCs displayed prolonged retention in blood, enhanced tumor targeting ability but reduced accumulation in liver and spleen.

3.10. In vivo anti-tumor activity

As shown in Fig. 9A, body weight of mice treated with BSA-NLCs and BSA-AL-NLCs increased more than that of Taxol group though without significant distinction, suggested less influence on

Table 1
AUC_{0-t} (μg/(g h)) in various tissues after i.v. injection of Taxol, BSA-NLCs, and BSA-AL-NLCs at a dose of 15 mg/kg PTX into S180 tumor-bearing mice. Results are shown as mean ± S.D ($n = 3$).

Tissue	Taxol	BSA-NLCs	BSA-AL-NLCs
Plasma	33.25 ± 4.32	18.72 ± 0.94*	46.73 ± 4.21**
Heart	56.51 ± 5.48	11.44 ± 1.92*	15.05 ± 1.99*
Liver	229.90 ± 28.39	484.80 ± 86.78*	173.73 ± 19.98
Spleen	79.14 ± 16.62	155.55 ± 31.27*	61.63 ± 12.14
Lung	69.48 ± 11.33	18.02 ± 3.57*	19.11 ± 0.76*
Kidney	73.11 ± 8.85	51.11 ± 6.64*	46.81 ± 10.39*
Tumor	15.92 ± 3.66	20.18 ± 4.26	46.96 ± 5.49**

* $P < 0.05$, versus Taxol.
** $P < 0.05$, versus Taxol and BSA-NLCs.

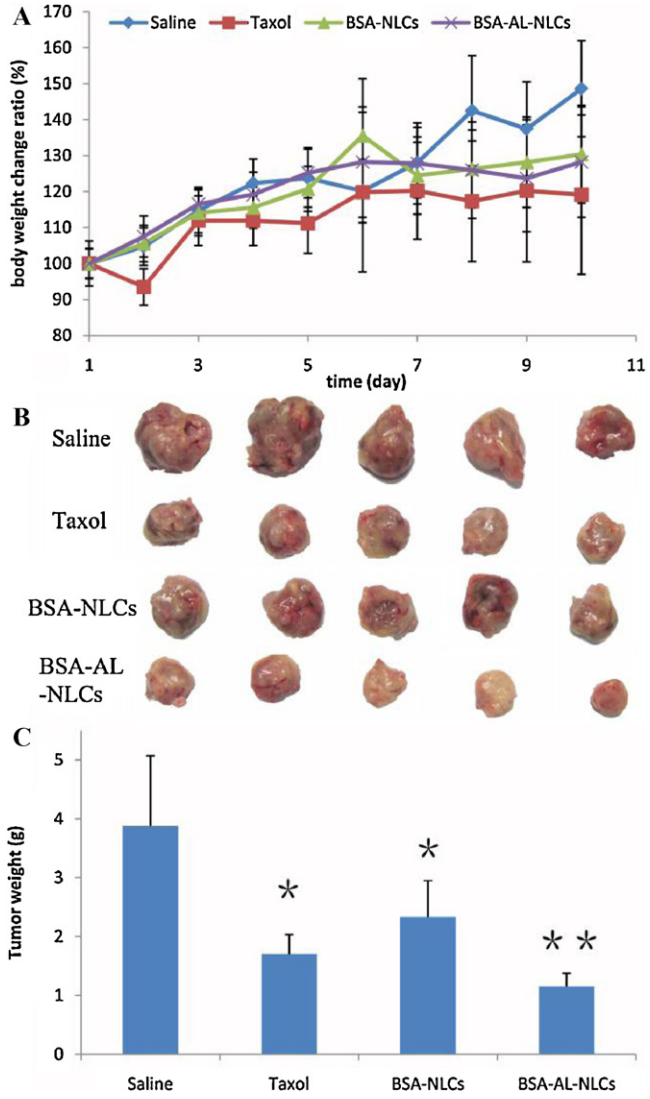

Fig. 9. Change ratio of body weight (A), tumor graph (B) and tumor weight (C) of tumor-bearing mice after i.v. application of different PTX preparation (*$P < 0.05$, versus Saline group; **$P < 0.05$, versus Saline, Taxol and BSA-NLCs group).

body weight. The final tumor images and weight were exhibited in Fig. 9B and C. Judging from Fig. 9B, the tumor inhibition efficacy in a descending order was BSA-AL-NLCs > Taxol > BSA-NLCs > Saline. The tumor weight of mice treated with Saline, Taxol, BSA-NLCs and BSA-AL-NLCs was 3.88 ± 1.19 g, 1.70 ± 0.56 g, 2.09 ± 0.34 g and 1.15 ± 0.22 g, respectively. It could be drawn that BSA-AL-NLCs inhibited tumor growth more effectively than Taxol and BSA-NLCs ($P < 0.05$), with the TIR of 70.31%. While, Taxol exhibited slightly better tumor inhibition efficacy than BSA-NLCs without statistically significant ($P > 0.05$), with the TIR of 56.05% compared to 46.04%.

4. Discussion

The pH-sensitive protonatable hydrophilic head and hydrophobic chain of AL seemed a unique combination for its pH-sensitive membranolysis (Chen et al., 2009a,b; Ho et al., 2011). The optimization of polyanions suggested that hydrophobic modification improved their membranolytic activities, confirmed the importance of hydrophobic residues in their membranolysis. Other researchers found that pH-dependent protonation of the hydrophilic residues played an important role in pH-sensitive membrane disruption of polymalic acid peptide, suggested that the improved affinity with membrane at lower pH was vital to induce pH-sensitive lysis of membrane (Ding et al., 2011). At neutral pH, AL burdened little H^+ and only exhibited weak membranolysis even at high concentration due to its weaker affinity with membranes. At lower pH, AL adsorbed more H^+ and became more positive charged. So the electrostatic affinity with negative charged biomembrane became stronger at lower pH, facilitating the insertion of its hydrophobic chain into biomembranes and the disturbance of membrane and the final disruption. Therefore, AL exhibited particular interest to develop endo/lysosomolytic nanocarriers.

It was widely accepted that nanoparticles with strong positive charge suffered from opsonin binding and RES recognition, resulted fast clearance from blood by RES (Li et al., 1999; Zelphati et al., 1998). In this study, BSA, a negative charged protein at neutral pH, was added to coat on AL-NLCs and shield its strong net positive charge (Jung et al., 2010) to increase the stability in blood and prolong the resistance time for the following study. Of course, other materials which can shield the positive charge of AL-NLCs can also be chosen to replace BSA.

According to the conclusions previously reported, nanoparticles smaller than 200 nm preferred to accumulated in tumor tissues due to the enhanced permeability and retention (EPR) effect (Duncan et al., 1996), and nanoparticles smaller than 100 nm could avoid the recognition of reticuloendothelial system and exhibited longer blood circulation effect (Gaur et al., 2000). The slight difference of size in this study would not induce distinction of their fate in vivo and in cells. The CLSM images also displayed amounts of lysosomes in cells after incubated with either of the NLCs for 1 h, indicating all the NLCs entered cells via endosome–lysosome path. In addition, all the prepared particles meet the widely accepted requirement of size to avoid the opsonin binding and RES recognition and facilitate tumor targeting.

BSA-AL-NLCs unsurprisingly acquired pH-sensitive membranolytic activity via insertion of AL. What is more, in contrast to AL, BSA-AL-NLCs showed almost negligible hemolytic activity at pH 7.4 even at high concentration, indicating the safety of BSA-AL-NLCs to biomembranes at neutral pH. BSA-AL-NLCs were membranolytic only at acidic pH typical of lysosomes, thus devoid of cytotoxicity and are expectable used as lysosomolytic drug delivery system. The details and mechanism of its pH-sensitive membranolysis are under research.

In contrast to pH-independent release of PTX from BSA-NLCs, BSA-AL-NLCs released PTX pH-dependently, which was ascribed to the BSA layer of BSA-AL-NLCs and the pH-dependent BSA ablation from BSA-AL-NLCs. BSA was water-soluble protein and formed a hydrophilic battle for the diffusion of hydrophobic PTX from NLCs. At pH milieu of endo/lysosome, BSA ablated from BSA-AL-NLCs for the decreased electrostatic attraction between less negative charged BSA and AL-NLCs, resulted the removement of the diffusion battle and the increased release. Of particular interest, pre-treatment of BSA-AL-NLCs with PBS of pH 5.4 for 1 h increased the total cumulative release amount of PTX at pH 7.4, suggesting the temporary entrapment in lysosomal pH could promote the release of PTX from BSA-AL-NLCs. This pH-dependent release profiles was attracted for the lysosomolytic drug delivery.

Calcein undergo self-quenching in lysosomal acid environment. This quenching effect could be reduced when released from lysosome and dispersed in the cytoplasm, and thus exhibited green fluorescence when excited with laser (Ho et al., 2011). In contrast to BSA-NLCs, AL-NLCs and BSA-AL-NLCs disrupted lysosome and diffused into cytoplasm timely, indicating both AL-NLCs and BSA-AL-NLCs acquired lysosomolytic capability by inserting pH-sensitive membranolytic AL. This proved that AL could be used to prepare lysosomolytic nanoparticles via convenient insertion, and the BSA layer did not affect the lysosomolytic activity

compared with AL-NLCs. This may provide a convenient method to build more nanoparticles with lysosomolytic capability and used as extra lysosomal drug delivery systems. The lysosome disruption and cytoplasmic trafficking mechanism will be studied in our following research.

Compared with BSA-NLCs, BSA-AL-NLCs did not present obvious toxic effect on MCF-7 cells even at the highest concentration, indicating the weak positive charge of BSA-AL-NLCs had no influence on cell viability. As expected, PTX-loaded BSA-AL-NLCs inhibited the proliferation more effective in comparison with BSA-NLCs. BSA-AL-NLCs disrupted the membrane of lysosome and diffused to cytoplasm quickly after endocytosis, facilitated drug targeting and inhibited the proliferation. While BSA-NLCs was entrapped in lysosome for lacking the ability of lysosomolysis, resulting little cytoplasmic diffusion of PTX and the final low anti-tumor effect in vitro. It is obviously that the lysosomolytic activity facilitated lysosomal escape of BSA-AL-NLCs and cytoplasmic release of PTX to inhibit the proliferation of cancer cells.

Without BSA layer on the surface, BSA-NLCs would be recognized and cleared by reticuloendothelial system (RES) and resulted short residence time in blood. BSA-NLCs phagotrophic by RES were transferred to and accumulated in RES-rich organs (Kweon et al., 2010; Xiao et al., 2011), liver and spleen, but less in tumor for the reduced passive target ability caused by the rapid clearance from blood. Coating BSA on nanoparticles could increase the stability in plasma and prolong the residence time in vivo (Furumoto et al., 2007; Quan et al., 2011). BSA-AL-NLCs exhibited more effective tumor targeting capability than BSA-NLCs, for the BSA layer of BSA-AL-NLCs prolonged the residence time in blood and increased the opportunity of BSA-AL-NLCs accumulated in tumor due to EPR effect. Besides, the accumulation ability of BSA in tumor (Felix, 2008; Stehle et al., 1997) may also contribute to the increased tumor targeting ability of BSA-AL-NLCs than BSA-NLCs.

In vivo anti-tumor activity confirmed the better tumor inhibition efficacy of BSA-AL-NLCs. This improved anti-tumor efficacy was due to the combination of increased PTX accumulation and effective lysosomal escape capability of BSA-AL-NLCs. BSA-NLCs presented less effective anti-tumor activity than Taxol even PTX concentration was higher after 2 h of injection, for BSA-NLCs were still entrapped in lysosomes and PTX could not release to cytoplasm. Overall, lysosomolytic BSA-AL-NLCs displayed expectable perspective to be used as tumor targeting and extra lysosomal anticancer drug delivery system.

5. Conclusions

Herein, AL, a pH-sensitive membrane disruptional agent, was successfully synthesized and used to prepare its composed nanoparticles (BSA-AL-NLCs) via convenient method. BSA-AL-NLCs possessed regular, spherical morphous, favorable particle size and zeta potential. BSA-AL-NLCs acquired pH-sensitive membranolytic activity of AL and were membranolytic only at acidic pH typical of lysosomes, thus devoid of cytotoxicity under physiological environment. The release of PTX from BSA-AL-NLCs was pH-dependent. BSA-AL-NLCs exhibited lysosomolytic capability in cells after endocytosis, promoting lysosomal escape of the delivery systems and drug release in cytoplasm. PTX-loaded BSA-AL-NLCs showed increased cytotoxicity than BSA-NLCs, due to its effective lysosomolytic capability. BSA-AL-NLCs presented better tumor targeting and In vivo anti-cancer activity.

Furthermore, this described method may provide an available and flexible platform to design and prepare more nanoparticles with lysosomolytic capability and used as extra lysosomal drug delivery systems (such as liposomes, micelles) to improve the therapeutical efficiency of loaded active agents, without unspecific plasma membrane permeation or membrane damage induced by free lysosomolytic agents. The details and mechanism of pH-sensitive membranolysis and lysosomolysis of BSA-AL-NLCs are under research and will be described in the following study.

Acknowledgements

This work was financially supported by Fundamental Research Funds for the Central Universities (JKY2009010 and JKQ2009005), the major project of the National Science and Technology of China for new drugs development (2009ZX09503-028) and grants from the National Natural Science Foundation of China (No. 81001414). The authors acknowledge Dr. Ayman (China Pharmaceutical University) for his kind editorial help in revising the English of this article.

References

Boussif, O., Lezoualc'h, F., Zanta, M.A., Mergny, M.D., Scherman, D., Demeneix, B., Behr, J.P., 1995. A versatile vector for gene and oligonucleotide transfer into cells in culture and in vivo: polyethylenimine. Proc. Natl. Acad. Sci. U. S. A. 92, 7297–7301.

Chen, R., Khormaee, S., Eccleston, M.E., Slater, N.K.H., 2009a. Effect of L-leucine graft content on aqueous solution behavior and membrane-lytic activity of a pH-responsive pseudopeptide. Biomacromolecules 10, 2601–2608.

Chen, R., Khormaee, S., Eccleston, M.E., Slater, N.K.H., 2009b. The role of hydrophobic amino acid grafts in the enhancement of membrane-disruptive activity of pH-responsive pseudo-peptides. Biomaterials 30, 1954–1961.

Chen, R., Yue, Z., Eccleston, M.E., Slater, N.K.H., 2008. Aqueous solution behaviour and membrane disruptive activity of pH-responsive PEGylated pseudo-peptides and their intracellular distribution. Biomaterials 29, 4333–4340.

Ding, H., Portilla-Arias, J., Patil, R., Black, K.L., Ljubimova, J.Y., Holler, E., 2011. The optimization of polymalic acid peptide copolymers for endosomolytic drug delivery. Biomaterials 32, 5269–5278.

Duncan, R., Connors, T.A., Meada, H., 1996. Drug targeting in cancer therapy: the magic bullet, what next? J. Drug Target. 3, 317–319.

Eccleston, M.E., Kuiper, M., Gilchrist, F.M., Slater, N.K.H., 2000. pH-responsive pseudo-peptides for cell membrane disruption. J. Control. Release 69, 297–307.

Felix, K., 2008. Albumin as a drug carrier: design of prodrugs, drug conjugates and nanoparticles. J. Control. Release 132, 171–183.

Fischer, D., Bieber, T., Li, Y., Elsässer, H.-P., Kissel, T., 1999. A novel non-viral vector for DNA delivery based on low molecular weight, branched polyethylenimine. Effect of molecular weight on transfection efficiency and cytotoxicity. Pharm. Res. 16, 1273–1279.

Furumoto, K., Yokoe, J.-I., Ogawara, K.-i., Amano, S., Takaguchi, M., Higaki, K., Kai, T., Kimura, T., 2007. Effect of coupling of albumin onto surface of PEG liposome on its in vivo disposition. Int. J. Pharm. 329, 110–116.

Gaur, U., Sahoo, S.K., De, T.K., Ghosh, P.C., Maitra, A., Ghosh, P.K., 2000. Biodistribution of fluoresceinated dextran using novel nanoparticles evading reticuloendothelial system. Int. J. Pharm. 202, 1–10.

Ho, V.H.B., Slater, N.K.H., Chen, R., 2011. pH-responsive endosomolytic pseudopeptides for drug delivery to multicellular spheroids tumour models. Biomaterials 32, 2953–2958.

Jones, R.A., Cheung, C.Y., Black, F.E., Zia, J.K., Stayton, P.S., Hoffman, A.S., Wilson, M.R., 2003. Poly(2-alkylacrylic acid) polymers deliver molecules to the cytosol by pH-sensitive disruption of endosomal vesicles. Biochem. J. 372, 65–75.

Jung, S.H., Kim, S.K., Jung, S.H., Kim, E.H., Cho, S.H., Jeong, K.-S., Seong, H., Shin, B.C., 2010. Increased stability in plasma and enhanced cellular uptake of thermally denatured albumin-coated liposomes. Colloids Surf. B: Biointerfaces 76, 434–440.

Khormaee, S., Chen, R., Park, J.K., Slater, N.K.H., 2010. The influence of aromatic side-chains on the aqueous properties of pH-sensitive poly(L-lysine iso-phthalamide) derivatives. J. Biomater. Sci. Polym. Ed. 21, 1573–1588.

Kichler, A., Leborgne, C., Coeytaux, E., Danos, O., 2001. Polyethylenimine-mediated gene delivery: a mechanistic study. J. Gene Med. 3, 135–144.

Kim, E.-M., Jeong, H.-J., Park, I.-K., Cho, C.S., Bom, H.-S., Kim, C.-G., 2004. Monitoring the effect of PEGylation on polyethylenimine in vivo using nuclear imaging technique. Nucl. Med. Biol. 31, 781–784.

Kweon, S., Lee, H.-J., Hyung, W., Suh, J., Lim, J., Lim, S.-J., 2010. Liposomes coloaded with iopamidol/lipiodol as a RES-targeted contrast agent for computed tomography imaging. Pharm. Res. 27, 1408–1415.

Li, S., Tseng, W.C., Stolz, D.B., Wu, S.P., Watkins, S.C., Huang, L., 1999. Dynamic changes in the characteristics of cationic lipidic vectors after exposure to mouse serum: implications for intravenous lipofection. Gene Ther. 6, 585–594.

Martin, M., Rice, K., 2007. Peptide-guided gene delivery. AAPS J. 9, E18–E29.

Masotti, A., Moretti, F., Mancini, F., Russo, G., Di Lauro, N., Checchia, P., Marianecci, C., Carafa, M., Santucci, E., Ortaggi, G., 2007. Physicochemical and biological study of selected hydrophobic polyethylenimine-based polycationic liposomes and their complexes with DNA. Bioorg. Med. Chem. 15, 1504–1515.

Meyer, M., Zintchenko, A., Ogris, M., Wagner, E., 2007. A dimethylmaleic acid–melittin-polylysine conjugate with reduced toxicity, pH-triggered endosomolytic activity and enhanced gene transfer potential. J. Gene Med. 9, 797–805.
Mui, B., Ahkong, Q.F., Chow, L., Hope, M.J., 2000. Membrane perturbation and the mechanism of lipid-mediated transfer of DNA into cells. Biochim. Biophys. Acta 1467, 281–292.
Paillard, A., Hindré, F., Vignes-Colombeix, C., Benoit, J.-P., Garcion, E., 2010. The importance of endo-lysosomal escape with lipid nanocapsules for drug subcellular bioavailability. Biomaterials 31, 7542–7554.
Quan, Q., Xie, J., Gao, H., Yang, M., Zhang, F., Liu, G., Lin, X., Wang, A., Eden, H.S., Lee, S., Zhang, G., Chen, X., 2011. HSA coated iron oxide nanoparticles as drug delivery vehicles for cancer therapy. Mol. Pharmacol. 8, 1669–1676.
Sahay, G., Alakhova, D.Y., Kabanov, A.V., 2010. Endocytosis of nanomedicines. J. Control. Release 145, 182–195.
Singh, R., Al-Jamal, K.T., Lacerda, L., Kostarelos, K., 2008. Nanoengineering artificial lipid envelopes around adenovirus by self-assembly. ACS Nano 2, 1040–1050.
Smith, P.K., Krohn, R.I., Hermanson, G.T., Mallia, A.K., Gartner, F.H., Provenzano, M.D., Fujimoto, E.K., Goeke, N.M., Olson, B.J., Klenk, D.C., 1985. Measurement of protein using bicinchoninic acid. Anal. Biochem. 150, 76–85.
Stehle, G., Sinn, H., Wunder, A., Schrenk, H.H., Stewart, J.C.M., Hartung, G., Maier-Borst, W., Heene, D.L., 1997. Plasma protein (albumin) catabolism by the tumor itself—implications for tumor metabolism and the genesis of cachexia. Crit. Rev. Oncol./Hematol. 26, 77–100.
Tzeng, S.Y., Guerrero-Cázares, H., Martinez, E.E., Sunshine, J.C., Quiñones-Hinojosa, A., Green, J.J., 2011. Non-viral gene delivery nanoparticles based on Poly(β-amino esters) for treatment of glioblastoma. Biomaterials 32, 5402–5410.
Van den Bossche, J., Al-Jamal, W.T., Yilmazer, A., Bizzarri, E., Tian, B., Kostarelos, K., 2011. Intracellular trafficking and gene expression of pH-sensitive, artificially enveloped adenoviruses in vitro and in vivo. Biomaterials 32, 3085–3093.
Vanić, Z., Barnert, S., Süss, R., Schubert, R., 2011. Fusogenic activity of PEGylated pH-sensitive liposomes. J. Liposome Res., 1–10.
Wang, G.-J., Lai, T.-C., Chen, C., 2004. Inhibitory effects of L-arginine derivatives on endothelium-dependent vasorelaxing response to acetylcholine of the rat aorta. Eur. J. Med. Chem. 39, 611–617.
Wang, T., Yang, S., Petrenko, V.A., Torchilin, V.P., 2010. Cytoplasmic delivery of liposomes into MCF-7 breast cancer cells mediated by cell-specific phage fusion coat protein. Mol. Pharmacol. 7, 1149–1158.
Wang, X.-L., Ramusovic, S., Nguyen, T., Lu, Z.-R., 2007. Novel polymerizable surfactants with pH-sensitive amphiphilicity and cell membrane disruption for efficient siRNA delivery. Bioconjug. Chem. 18, 2169–2177.
Wang, X.-L., Xu, R., Lu, Z.-R., 2009. A peptide-targeted delivery system with pH-sensitive amphiphilic cell membrane disruption for efficient receptor-mediated siRNA delivery. J. Control. Release 134, 207–213.
Xiao, K., Li, Y., Luo, J., Lee, J.S., Xiao, W., Gonik, A.M., Agarwal, R.G., Lam, K.S., 2011. The effect of surface charge on in vivo biodistribution of PEG-oligocholic acid based micellar nanoparticles. Biomaterials 32, 3435–3446.
Xu, R., Wang, X.-L., Lu, Z.-R., 2010a. New amphiphilic carriers forming pH-sensitive nanoparticles for nucleic acid delivery. Langmuir 26, 13874–13882.
Xu, Y., Jin, X., Ping, Q., Cheng, J., Sun, M., Cao, F., You, W., Yuan, D., 2010b. A novel lipoprotein-mimic nanocarrier composed of the modified protein and lipid for tumor cell targeting delivery. J. Control. Release 146, 299–308.
Yessine, M.-A., Leroux, J.-C., 2004. Membrane-destabilizing polyanions: interaction with lipid bilayers and endosomal escape of biomacromolecules. Adv. Drug Deliv. Rev. 56, 999–1021.
Zelphati, O., Uyechi, L.S., Barron, L.G., Szoka Jr., F.C., 1998. Effect of serum components on the physico-chemical properties of cationic lipid/oligonucleotide complexes and on their interactions with cells. Biochim. Biophys. Acta 1390, 119–133.